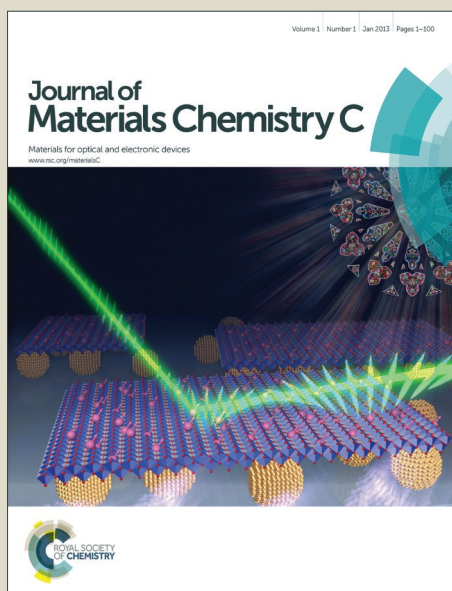


Journal of Materials Chemistry C

Accepted Manuscript



This is an *Accepted Manuscript*, which has been through the Royal Society of Chemistry peer review process and has been accepted for publication.

Accepted Manuscripts are published online shortly after acceptance, before technical editing, formatting and proof reading. Using this free service, authors can make their results available to the community, in citable form, before we publish the edited article. We will replace this *Accepted Manuscript* with the edited and formatted *Advance Article* as soon as it is available.

You can find more information about *Accepted Manuscripts* in the [Information for Authors](#).

Please note that technical editing may introduce minor changes to the text and/or graphics, which may alter content. The journal's standard [Terms & Conditions](#) and the [Ethical guidelines](#) still apply. In no event shall the Royal Society of Chemistry be held responsible for any errors or omissions in this *Accepted Manuscript* or any consequences arising from the use of any information it contains.

ARTICLE

The Controlled Deposition of $\text{Cu}_2(\text{Zn}_y\text{Fe}_{1-y})\text{SnS}_4$, $\text{Cu}_2(\text{Zn}_y\text{Fe}_{1-y})\text{SnSe}_4$ and $\text{Cu}_2(\text{Zn}_y\text{Fe}_{1-y})\text{Sn}(\text{S}_x\text{Se}_{1-x})_4$ Thin Films by AACVD: Potential Solar Cell Materials based on Earth Abundant Elements

Cite this: DOI: 10.1039/x0xx00000x

Received 00th January 2012,
Accepted 00th January 2012

DOI: 10.1039/x0xx00000x

www.rsc.org/

Punarja Kevin,^a Mohammad Azad Malik,^{*b} Paul O'Brien^{*a,b}

Highly crystalline thin films of $\text{Cu}_2(\text{Zn}_y\text{Fe}_{1-y})\text{SnS}_4$ (CZFTS), $\text{Cu}_2(\text{Zn}_y\text{Fe}_{1-y})\text{SnSe}_4$ (CZFTSe) and $\text{Cu}_2(\text{Zn}_y\text{Fe}_{1-y})\text{Sn}(\text{S}_x\text{Se}_{1-x})_4$ (CZFTS_xSe_{1-x})₄ (CZFTS_xSe_{1-x})₄) have been deposited by Aerosol Assisted Chemical Vapour Deposition (AACVD) from mixtures of dithio- or diseleno-carbamato, diselenophosphinato and acetylacetonato complexes. The structure, morphology, composition, optical and electrical properties of the deposited materials were investigated. The [Zn]:[Fe] and [S]:[Se] ratios are the important factors affecting the overall properties of these materials and can be controlled.

Introduction

Kesterite materials are considered to be amongst the better of the new absorbers for polycrystalline PV-solar cells.¹ The parent family encompasses $\text{Cu}_2\text{ZnSnS}_4$ (CZTS Kesterite), $\text{Cu}_2\text{ZnSn}(\text{S}_x\text{Se}_{1-x})_4$, (CZTS_xSe_{1-x})₄ and $\text{Cu}_2\text{ZnSnSe}_4$ (CZTSe).¹ The related iron containing phases $\text{Cu}_2(\text{Zn}_y\text{Fe}_{1-y})\text{SnS}_4$ (CZFTS), $\text{Cu}_2(\text{Zn}_y\text{Fe}_{1-y})\text{SnSe}_4$ (CZFTSe) and (CZFTS_xSe_{1-x})₄ have optical band gaps, large absorption coefficient and transport properties similar to those of CZTS.²⁻⁴ There are few studies reported for materials that can form in both the kesteritic (space group I48m) and the stannitic (space group I42m) type dependent upon the [Zn]:[Fe] ratio.⁴ The polymorphs have very small difference in thermodynamic stability. The addition of iron into CZTS thin films decreases the optical band gap which can improve the Power Conversion Efficiency (PCE) of Thin Film Solar Cells (TFSCs). The solubility of iron in the CZTS derivatives plays a key role in controlling many parameters.⁵

The iron containing analogues are of particular interest for Si-based tandem solar cells as the lattice constant of Si (5.4311 Å) lies between two end members in the $\text{Cu}_2(\text{Zn}_y\text{Fe}_{1-y})\text{Sn}(\text{S}_x\text{Se}_{1-x})_4$ series CZTS (5.414 Å) to CZTSe (5.435 Å). Variations in [Zn]:[Fe], or [S]:[Se] composition affect both the lattice spacing's and band gap.²⁻⁶ The magnetic⁵ and vibrational⁷ properties of CZFTS alloys have also been investigated. Addition of Fe in CZTS thin films decreases the optical band gap energy which can improve the PCE of TFSCs.² Nanocrystals of the related $\text{CuIn}_x\text{Ga}_{1-x}(\text{S}_y\text{Se}_{1-y})_2$ (CIGSSe) synthesized by colloidal methods, have band gaps tunable from 0.98 - 2.40 with changes in x and y from 0 to 1.⁸

AACVD is a simple technique which can operate at an ambient-pressure using the nebulization of the precursor molecules, followed

by transport of the aerosol by an inert carrier gas such as argon or nitrogen to a substrate surface heated in a furnace where thermal decomposition of the precursor occurs.

AACVD has been widely applied in the deposition of complex systems and has enabled the use of less volatile precursors than more conventional CVD methods. These have included high temperature superconductors⁹ and other oxides.⁹ Stoichiometry controlled thin films of CdS, ZnS, and $\text{Cd}_{1-x}\text{Zn}_x\text{S}$ were deposited from $\text{Cd}(\text{SOCCH}_3)_2$ -TMEDA and $\text{Zn}(\text{SOCCH}_3)_2$ -TMEDA (TMEDA = N,N,N,N-tetramethylethylenediamine).⁹ Marks *et al.* reported the deposition of metallic silver thin films using tris(phosphino)boratosilver(I) complexes¹⁰ and Parkin *et al.* reported a single step route to the deposition of super hydrophobic surfaces through AACVD and deposition of ZnO thin films by AACVD.¹¹ Wijayantha *et al.* reported the polycrystalline a- Fe_2O_3 electrodes by aerosol-assisted chemical vapour deposition from a ferrocene precursor.¹² Mazhar *et al.* reported the deposition of high quality NiTiO_3 thin films from a single-source heterobimetallic complex $[\text{Ni}_2\text{Ti}_2(\text{OEt})_2(\text{m-OEt})_6(\text{acac})_4]$ precursor.¹³ The method has also been successfully applied for α - Fe_2O_3 using $[\text{Fe}_6(\text{PhCOO})_{10}(\text{acac})_2(\text{O})_2(\text{OH})_2]_3\text{C}_7\text{H}_8$.¹⁴ AACVD has recently been used for the deposition of various semiconductor materials including SnS,¹⁵ CZTS,¹⁶ CuInSe_2 ,¹⁷ CuGaSe_2 ,¹⁷ $\text{CuIn}_{0.7}\text{Ga}_{0.3}\text{Se}$,¹⁷ MoS_2 ,¹⁸ inorganic-organic perovskite $(\text{CH}_3\text{NH}_3)\text{PbBr}_3$,¹⁹ SnSe and Cu_2SnSe_3 .¹⁹ Hassan *et al.* reported different morphologies of hexagonal FeSe from 1-benzoyl-3-(4-ferrocenylphenyl)selenourea under the influence of surfactants (span and triton) and temperature.²⁰ Very recently bismuth vanadate (BiVO_4) thin film photoelectrodes prepared by AACVD on fluorine doped tin oxide (FTO) glass substrates were produced., BiVO_4 photoelectrodes is promising for use in PEC water-splitting cells.²¹ Recently the

application of AACVD has been reviewed by Marchand et al.⁹ β - In_2S_3 thin films deposited by AACVD, irrespective of different metal ligand design, generate comparable morphologies of thin films at different temperatures, the measured photoelectrochemical performance of these films were highly useful in fabricating electrodes for solar energy harvesting and optoelectronic application.²²

Dhurba and reported the deposition of CZFTS thin films, by spray pyrolysis followed by sulfurization at ~ 500 °C.⁷ Agwane *et al.* reported the effect of [Zn]:[Fe] ratio on the properties of CZFTS thin films deposited by a pulsed laser deposition technique but the formation of Cu-rich and Zn-poor large grains was found to affect these parameters.² We have used a series of molecular precursors for the deposition of binary and ternary materials.²² Herein, we report the AACVD of CZFTS, CZFTSe and CZFTSSe thin films and detailed investigation on the effect of [Zn]:[Fe] and [S]:[Se] ratios on the structure, morphology, optical band gap and electrical resistance of these materials.

Experimental Section

Preparations were performed under an inert atmosphere of dry nitrogen using standard Schlenk techniques. All reagents were purchased from Sigma-Aldrich chemical company and used as received. Solvents were distilled prior to use. Elemental analysis was performed by the University of Manchester micro-analytical laboratory. TGA measurements were carried out by a Seiko SSC/S200 model from 10 to 600 °C with a heating rate of 10 °C/min under nitrogen. Melting point was recorded on a Stuart melting point apparatus and uncorrected.

Synthesis of metal-organic complexes

The compounds $[\text{Cu}(\text{S}_2\text{CNET}_2)_2]$, $[\text{Fe}(\text{S}_2\text{CNET}_2)_3]$, $[\text{Bu}_2\text{Sn}(\text{S}_2\text{CNET}_2)_2]$, $[\text{Zn}(\text{S}_2\text{CNET}_2)_2]$, $[\text{Zn}(\text{Se}_2\text{CNET}_2)_2]$ and $[\text{Cu}(\text{PPh}_3)(\text{Ph}_2\text{P}(\text{Se})\text{NP}(\text{Se})\text{Ph}_2)]$ were synthesised and recrystallized as reported in literature, brief details follow.^{14,23-25}

$[\text{Cu}(\text{S}_2\text{CNET}_2)_2]$: Sodium diethyldithiocarbamate (13 mmol) was dissolved in methanol in a 500 mL double necked round-bottom flask. Slow addition of a methanolic solution of $\text{Cu}(\text{NO}_3)_2$ (6.5 mmol) gave a black precipitate, which was isolated by filtration. Recrystallization was performed using chloroform. Yield: 4.78 g (73%), Mpt: 201 °C, IR ($\nu_{\text{max}}/\text{cm}^{-1}$): 2979(w), 2868(w), 1501(s), 1434(m), 1270(s), 1205(m) and 1144(m), Elemental analysis: Calc. for $\text{C}_{10}\text{H}_{20}\text{N}_2\text{S}_4\text{Cu}$: C, 33.4; H, 5.5; N, 7.7; S, 35.6; Cu, 17.6 %. Found: C, 33.2; H, 5.3; N, 7.3; S, 35.2; Cu, 17.2 %.

$[\text{Fe}(\text{S}_2\text{CNET}_2)_3]$: Sodium diethyldithiocarbamate (13 mmol) with $\text{Fe}(\text{NO}_3)_3$ (4 mmol) gave a black powder which on recrystallization produced black shiny crystals. yield 4.81 g (79%), Mpt: 198-201 °C, IR ($\nu_{\text{max}}/\text{cm}^{-1}$): 2967(w), 2938(w), 1478(s), 1429(m), 1352(w), 1296(w), 1296(m), 1270(s), 1050(s) and 950(s), Elemental analysis: Calc. for $\text{C}_{15}\text{H}_{30}\text{N}_3\text{S}_6\text{Fe}$: C, 35.98; H, 6.04; N, 8.39; S, 38.43; Fe, 11.15 %. Found: C, 35.7; H, 6.3; N, 8.4; S, 37.82; Fe, 11.0 %.

$[\text{Zn}(\text{S}_2\text{CNET}_2)_2]$: Produced by the reaction between zinc acetate (6.5 mmol) and Sodium diethyldithiocarbamate (13 mmol) as described above. The crude product was obtained was a white powder which on recrystallization from chloroform gave colourless crystals. Yield 4.81 g (79%), Mpt: 181 °C, IR ($\nu_{\text{max}}/\text{cm}^{-1}$): 2967(w), 2938(w), 1499(s), 1427(m), 1352(w), 1296(w), 1296(m), 1270(s), 1200(s) and 1143(s), Elemental analysis: Calc. for $\text{C}_{10}\text{H}_{20}\text{N}_2\text{S}_4\text{Zn}$: C, 33.1; H, 5.5; N, 7.7; S, 35.4; Zn, 18.1 %. Found: C, 32.7; H, 5.3; N, 7.4; S, 35.0; Zn, 18.0 %.

$[\text{Bu}_2\text{Sn}(\text{S}_2\text{CNET}_2)_2]$: The compound was synthesised as described before¹¹ using di-n-butylindichloride (6.5 mmol) and Sodium diethyldithiocarbamate (13 mmol). A white powdered product was isolated by vacuum filtration and recrystallized from a mixture of ethanol-chloroform, white shiny crystals obtained. Yield 5.5 g, (67%), Mpt: 57 °C, IR ($\nu_{\text{max}}/\text{cm}^{-1}$): 2953(w), 2924(w), 1483(s), 1456(m), 1417(s), 1353(m), 1298(m), 1253(s), 1205(s) and 1138(s), Elemental analysis: Calc. for $\text{C}_{18}\text{H}_{38}\text{N}_2\text{S}_4\text{Sn}$: C, 40.8; H, 7.2; N, 5.3; S, 24.2; Sn, 22.4 %. Found: C, 39.9; H, 7.5; N, 5.1; S, 22.8; Sn, 21.4 %.

$[\text{Zn}(\text{Se}_2\text{CNET}_2)_2]$: To a freshly prepared methanolic solution of $[\text{NaSeCH}_2\text{CH}_2\text{CH}_2\text{NMe}_2]$ a suspension of $\text{Zn}(\text{OAc})_2 \cdot 2\text{H}_2\text{O}$ (23.5 mmol) in 50 mL dichloromethane was added and stirred for 3 hours. A colourless solution thus obtained was dried by rotary evaporation. The residue was washed with hexane and extracted with toluene. NaOAc residue was filtered off and the collected filtrate on evaporation gave the corresponding creamy white solid. Yield: 46%. For ^1H NMR (CDCl_3) peaks obtained at 1.89 ($-\text{CH}_3$)₂CH group, 2.25 ($\text{N}(\text{CH}_3)_2$), 2.5 (NCH₂). Elemental analysis Calc. for $\text{C}_{10}\text{H}_{24}\text{N}_2\text{Se}_2\text{Zn}$: C, 30.3; H, 6.1; N, 7.1 % Found: C, 30.1; H, 5.9; N, 6.8 %

$[\text{Cu}(\text{PPh}_3)[\text{Ph}_2\text{P}(\text{Se})\text{NP}(\text{Se})\text{Ph}_2]$: In a 150 mL methanolic solution of 1.2 g (2.6 mmol) $\text{K}[\text{Ph}_2\text{P}(\text{Se})\text{NP}(\text{Se})\text{Ph}_2]$ was mixed with a solution of $[\text{Cu}(\text{PPh}_3)_2\text{NO}_3]$ (1.4 g, 2.1 mmol) in 100 mL methanol. Then stirred for 30 minutes and the precipitate was filtered, the filtrate on rotary evaporation gave a pinkish powder. The product was recrystallized from dichloromethane resulted pinkish crystals were dried and purified under vacuum. Yield: 64% $[\text{Cu}(\text{PPh}_3)[\text{Ph}_2\text{P}(\text{Se})\text{NP}(\text{Se})\text{Ph}_2]$; m. p; 221-223 °C. ^31P NMR (400 MHz, CDCl_3 , rel. to 85% H_3PO_4): $\delta = 26.14$ ppm with two P-Se satellites, 1JP-Se-576 Hz. IR ($\nu_{\text{max}}/\text{cm}^{-1}$): 3050 cm^{-1} (s) 1165 cm^{-1} (s) 1100, 755 (m), 690 (m) and 545 (m). Mass spec: m/z-869, 670, 460, 341. Elemental Analysis: Calc. for $\text{C}_{42}\text{H}_{35}\text{CuNP}_3\text{Se}_2$: C, 58.1; H, 4.1; N, 1.6% and Found; C, 57.87; H, 3.92; N, 1.48 %.

Deposition of thin films

The thin films were deposited using AACVD. Glass slides (1 x 2 cm) were used as substrates for the deposition of thin films. Substrates were thoroughly cleaned and sonicated in acetone for 30 minutes to remove any possible contamination. In a typical deposition experiment, precursor complex (or a suitable combination of precursors) was dissolved in 20 mL THF taken in a two-necked 100 mL round-bottom flask. The round-bottom flask was kept in a water bath above the piezoelectric modulator of a PIFCO ultrasonic humidifier (model 1077). The

ARTICLE

Sample	T (°C)	[Cu]	[Cu]	[Zn]	[Zn]	[Sn]	[Sn]	[Fe]	S	Se	a(Å)	c(Å)	a(Å)	BG/ eV	R/Ω
		AACVD	EDX	AACVD	EDX	AACVD	EDX	AACVD	EDX	EDX	EDX	Riet	Riet	hkl	
CZFTS(C1)	350	2.78	2.2	0.7	0.7	1.4	1.3	0.7	3.4	0	5.411(4)	10.862(3)	5.412(8)	1.72	2.48
CZFTS(C2)	350	2.78	1.9	0.4	0.3	1.4	1.3	1	3.2	0	5.418(7)	10.829(1)	5.415(2)	1.67	2.42
CZFTSse(C1)	350	2.78	1.7	0.7	0.6	1.4	0.8	0.7	1.9	1.2	x	x	5.477(5)	1.64	2.31
CZFTSse (C2)	350	2.78	2	0.7	0.4	1.4	0.8	1	2.1	1.7	x	x	5.429(8)	1.61	2.29
CZFTSe(C1)	350	2.78	2	0.7	0.7	1.4	1	0.7	0	3.1	x	x	5.429(7)	1.47	2.21
CZFTSe(C2)	350	2.78	1.8	0.4	0.3	1.4	0.9	1	0	3	x	x	5.492(7)	1.48	2.16

Table 1: Consolidated Table showing measured parameters (band gaps, resistance, EDX, lattice constants) and the concentrations of individual components in the precursor mixtures for Zn-rich (1) and Fe-rich (2) phases of CZFTS, CZFTSe and CZFTSse.

aerosol droplets of the precursor thus generated were transferred into the hot wall zone of the reactor by a carrier gas (Argon). The Argon flow rate was controlled at 180 sccm by a Platon flow gauge. Both the solvent and precursor were evaporated, and the precursor vapor reached the heated substrate surface where thin film was deposited at 300- 400 °C.

Deposition of CZFTS thin films

Thin films of $\text{Cu}_2(\text{Zn}_y\text{Fe}_{1-y})\text{SnS}_4$ (CZFTS) were deposited using a mixture of $[\text{Cu}(\text{S}_2\text{CNET}_2)_2]$ (2.78 mmol), $[\text{Fe}(\text{S}_2\text{CNET}_2)_3]$ (0.7 mmol), $[\text{Zn}(\text{S}_2\text{CNET}_2)_2]$ (0.7 mmol) and $[\text{Bu}_2\text{Sn}(\text{S}_2\text{CNET}_2)_2]$ (1.40 mmol) in the molar ratio 2 : 1 : 0.5 : 0.5 : 1 in 20 ml THF. The AACVD experiments were carried out as described above at 300 and 350 °C. The Fe-rich compositions of this material were deposited by increasing the ratio of the iron precursor as compared to that of zinc precursor. A mixture of $[\text{Cu}(\text{S}_2\text{CNET}_2)_2]$ (2.78 mmol), $[\text{Fe}(\text{S}_2\text{CNET}_2)_3]$ (1.0 mmol), $[\text{Zn}(\text{S}_2\text{CNET}_2)_2]$ (0.4 mmol) and $[\text{Bu}_2\text{Sn}(\text{S}_2\text{CNET}_2)_2]$ (1.40 mmol) in 2 : 1 : 0.7 : 0.3 : 1 molar ratio in 20 ml THF was used to deposit films at 350 °C.

Deposition of CZFTSe thin films

The deposition of $\text{Cu}(\text{ZnFe})\text{SnSe}_4$ was carried out by using a mixture of $[\text{Cu}(\text{PPh}_3)(\text{Ph}_2\text{P}(\text{Se})\text{NP}(\text{Se})\text{Ph}_2)]$ (2.78 mmol), $[\text{Sn}(\text{CH}_3\text{CO}_2)_4]$ (1.40 mmol) $[\text{Zn}(\text{Se}_2\text{CNET}_2)_2]$ (0.7 mmol) and $[\text{Fe}(\text{acac})_3]$ (0.7 mmol) in the molar ratio 2 : 1 : 0.5 : 0.5 : 1 in 20 mL of THF at 300 °C and 350 °C for 55 minutes. For the deposition of Fe-rich films a similar deposition was carried out at 350 °C with different ratio of $[\text{Zn}(\text{S}_2\text{CNET}_2)_2]$ (0.4 mmol) (2.8 mmol) and $[\text{Fe}(\text{acac})_3]$ (1.0 mmol) in 2 : 1 : 0.7 : 0.3 : 1 molar ratio in 20 mL THF and keeping other precursor concentrations same as in the previous experiment.

Deposition of CZFTSse thin films

The $\text{Cu}_2(\text{Zn}_y\text{Fe}_{1-y})\text{Sn}(\text{S}_x\text{Se}_{1-x})_4$ thin films were deposited by using $[\text{Zn}(\text{Se}_2\text{CNET}_2)_2]$ (0.7 mmol) whilst keeping all the other precursors same as for Zn-rich CZFTS (1: 0.5: 0.5: 1 in 20 mL of THF). The depositions were carried out at 300 °C and 350 °C. For the deposition of Fe-rich composition on the films, another deposition was carried out at 350 °C using $[\text{Zn}(\text{Se}_2\text{CNET}_2)_2]$ (0.4 mmol) and $[\text{Fe}(\text{S}_2\text{CNET}_2)_3]$ (1.0 mmol) in 2 : 1 : 0.7 : 0.3 : 1 molar ratio in 20 mL THF whilst keeping all the other concentrations same.

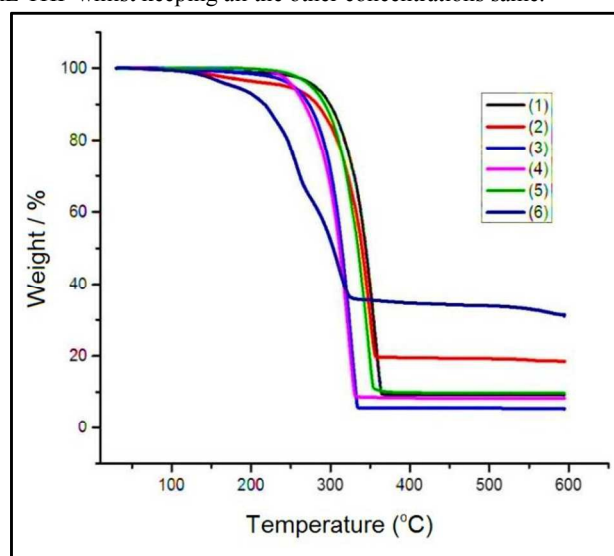


Figure 1: TGA of $[\text{Cu}(\text{S}_2\text{CNET}_2)_2]$ (1), $[\text{Fe}(\text{S}_2\text{CNET}_2)_3]$ (2), $[\text{Zn}(\text{S}_2\text{CNET}_2)_2]$ (3), $[\text{Bu}_2\text{Sn}(\text{S}_2\text{CNET}_2)_2]$ (4), $[\text{Zn}(\text{Se}_2\text{CNET}_2)_2]$ (5) and $[\text{Cu}(\text{PPh}_3)(\text{Ph}_2\text{P}(\text{Se})\text{NP}(\text{Se})\text{Ph}_2)]$ (6) complexes.

Characterisation of thin films

The p-XRD patterns were recorded on a Bruker D8 AXE diffractometer using Cu-K α radiations. The samples were mounted flat and scanned between 10 and 120° in a step size of 0.05 with a varying count rate depending upon the sample. The morphology and

microstructure of thin films were investigated by using a Philips XL 30 FEGSEM and film composition was studied by EDX analysis using a DX4 instrument at 20 KV with WD 10 mm. Raman spectra measurements taken in Renishaw 1000 Micro Raman system with an excitation wavelength of 520 nm, measurement range set from 100 to 700 cm⁻¹. UV-VIS measurement carried out in Perkin Elmer Lambda 1050 spectrophotometer (PSI), scanned across the range from 250–1000 nm. Electrical resistance measured using Jandel four probe conductivity meter under room temperature using 1 μ A current. TEM samples were prepared by evaporating a drop of a dilute suspension of the sample in toluene or hexane on carbon coated copper grid. The excess solvent was allowed to dry completely at room temperature. TEM images and elemental maps were collected on Technai T20 microscope using accelerating voltage of 300 kV. TEM (nanoscale) elemental maps were measured using Aztec software.

Results and Discussion

Thermal Decomposition Studies

Thermal decomposition studies were carried at 10–600 °C; heating rate 10 °C min⁻¹ under nitrogen. All compounds show rapid single step decomposition between 250–350 °C (Figure 1). The residual mass of [Fe(S₂CNET₂)₃] complex found to be about 18% which close to the calculated percentage of FeS (17.5%). The [Bu₂Sn(S₂CNET₂)₂] complex decomposed slightly faster than the other complexes and the residual mass found to be ~ 34 % which agrees with the calculated residual mass of SnS₂. [Zn(S₂CNET₂)₂] and [Zn(S₂CNET₂)₂] resulted with ~9–10 % residue which found to be half or less than half of the mass of the expected metal chalcogenides; ZnS (27 %) and ZnSe (20 %). TGA of [Cu(PPh₃)(Ph₂P(Se)NP(Se)Ph₂)] showed single step decomposition between 250 to 320 °C with residue ~ 10 % which was lesser than the expected residual mass of CuSe (16 %).

X-ray Diffraction Studies

The deposition of CZFTS materials at 300 °C gave very thin dark green films which did not diffract whereas black adherent films were deposited at 350 °C. The p-XRD pattern (Figure 2) of these films was corresponding to the Zn-rich phase of Cu₂Fe_{0.3}Zn_{0.7}Sn₁S₄ (ICDD 04-015-0225) with the tetragonal space group I-42m with lattice parameters a = 5.42 (2) Å and c = 10.86 (4) Å. Rietveld refinement carried out on the p-XRD patterns of the deposited material using this Zn-rich standard space group showed very good fit with a Rietveld parameter R_{wp} = 2.85, space group I-42m with lattice parameters a = 5.411 (4) Å and c = 10.862 (3) Å (Figure 3(a)). The main d-spacing for the planes were 3.13 Å (112), 1.91 Å (204), 1.91 Å (220), 1.63 Å (116) and 1.63 Å (312) respectively. The resultant d-spacing were well matched with the reported d-spacing for the corresponding planes at 3.13 Å (112), 1.91 Å (204), 1.91 Å (220),

1.63 Å (116) and 1.63 Å (312) respectively (ICDD: 04-015- 0225) for Cu₂Fe_{0.3}Zn_{0.7}Sn₁S₄. The doublet planes were not well resolved possibly due to broadening of the peaks due to the small size of the particles compared to the bulk materials, but the material is very close to cubic. The details of calculated d-spacings and 2 θ values are shown in Table S1 in the supplementary document. The lattice parameters also estimated calculated from the principal peaks in the p-XRD patterns to a cubic cell giving a = 5.412(8) Å in good agreement with the values obtained from the Rietveld refinement (Table 1). This approach was also used for all films some of which did not give good fits in the Rietveldt analysis.

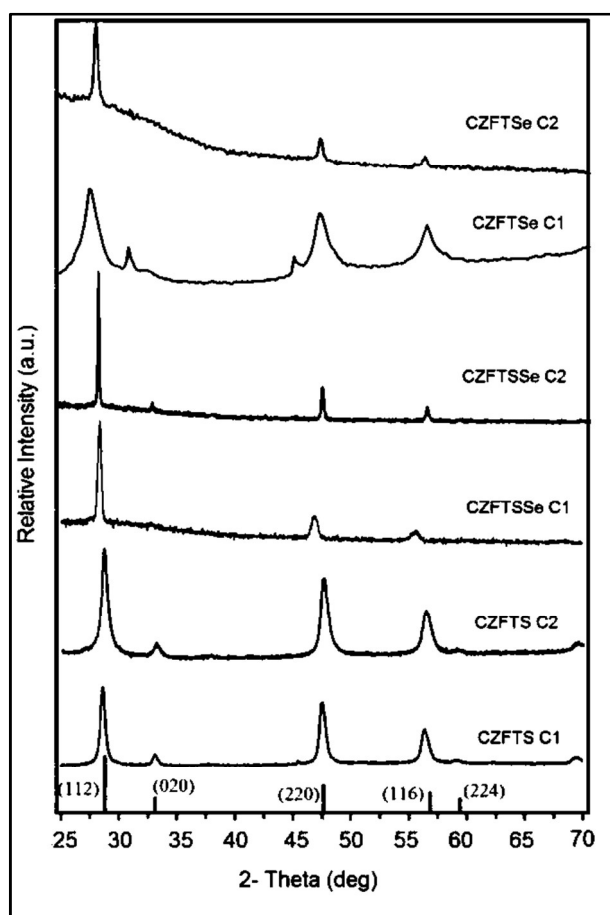


Figure 2: p-XRD patterns of Zn-rich (C1) and Fe-rich (C2) phases of CZFTS, CZFTSe, CZFTSse thin films deposited with different [Zn] at 350 °C.

CFTS films deposited at 350 °C using a higher ratio of the Fe precursor (CFTS C2 in Table 2) were very dark and uniform. The p-XRD pattern of as deposited films (Figure 3(b)) corresponds to the Fe-rich phase of Cu₂Fe_{0.7}Zn_{0.3}Sn₁S₄ (ICDD: 01-015-0228). No additional phase or impurities were found in the p-XRD and showed good match to the stick patterns can be seen in Figure 2. Rietveld refinement of the resultant p-XRD patterns analysed with the observed Fe-rich phase showed very good match with R_{wp} = 2.43 as shown in Figure 3(b). The standard material possesses an I-42m space group with space group number 12 and a = 5.43(2) Å and c = 10.79(4) Å and the refined space group was found to be I-42m with

lattice parameters $a = 5.42 \text{ \AA}$ and $c = 10.83 \text{ \AA}$. The resultant d-spacing for the planes and planes were 3.13 \AA (112), 1.91 \AA (220) and 1.63 \AA (312) which found to be the same as the standard d-spacing for the planes *i.e.* 3.13 \AA (112), 1.91 \AA (220) and 1.63 \AA (312)

respectively (ICDD: 01- 015- 0228). The details of calculated d-spacing's and 2θ positions are given in Table S2 in the supplementary document. The lattice parameters a calculated from the principal peaks in p-XRD patterns were $5.415(2)$ (see TableS1))

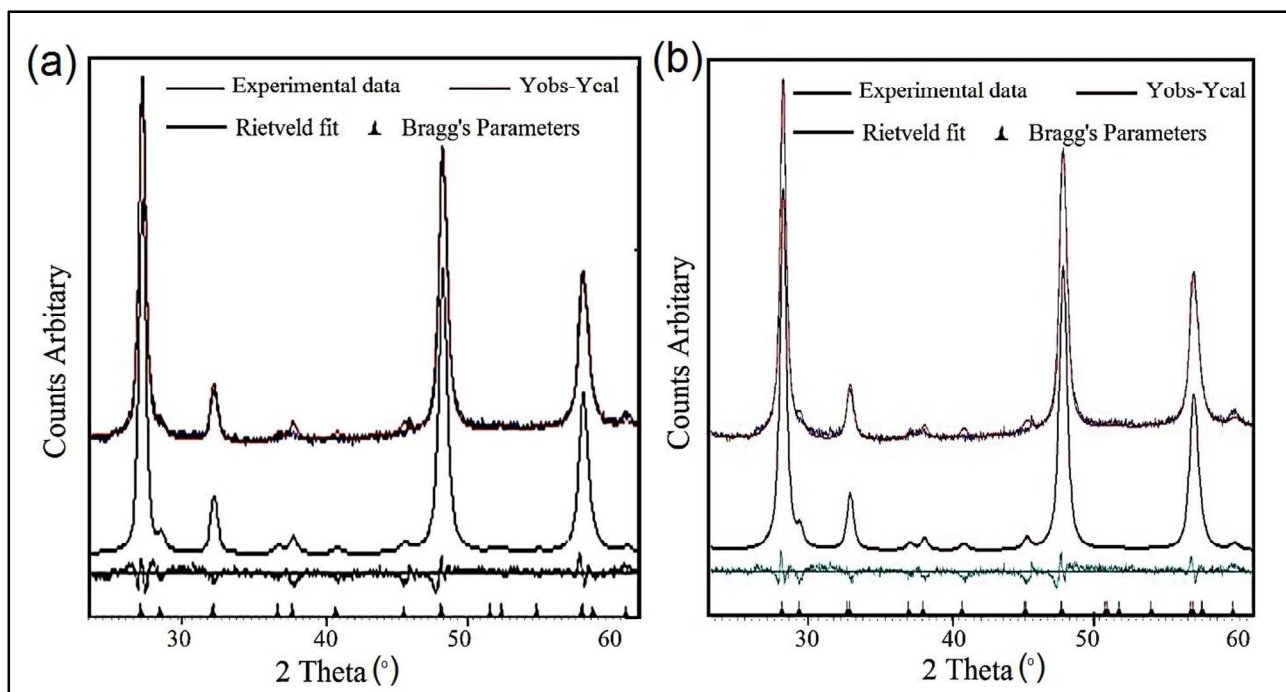


Figure 3: (a) Rietveld analysis p-XRD patterns of CZFTS thin films deposited at $350 \text{ }^\circ\text{C}$ using 2: 1: 0.5: 0.5: 1 of $[\text{Cu}(\text{S}_2\text{CNEt}_2)_2]$: $[\text{Fe}(\text{S}_2\text{CNEt}_2)_3]$: $[\text{Zn}(\text{S}_2\text{CNEt}_2)_2]$: $[\text{Bu}_2\text{Sn}(\text{S}_2\text{CNEt}_2)_2]$ precursors. The peaks fitted using $\text{Cu}_2\text{Fe}_{0.3}\text{Zn}_{0.7}\text{Sn}_1\text{S}_4$ (ICDD 04-015-0225) phase. (b) Rietveld analysis of p-XRD patterns of CZFTS thin films deposited at $350 \text{ }^\circ\text{C}$ using 2: 1: 0.7: 0.3: 1 of $[\text{Cu}(\text{S}_2\text{CNEt}_2)_2]$: $[\text{Fe}(\text{S}_2\text{CNEt}_2)_3]$: $[\text{Zn}(\text{S}_2\text{CNEt}_2)_2]$: $[\text{Bu}_2\text{Sn}(\text{S}_2\text{CNEt}_2)_2]$ precursors. The peaks fitted using Fe-rich $\text{Cu}_2\text{Fe}_{0.7}\text{Zn}_{0.3}\text{Sn}_1\text{S}_4$ (ICDD: 01-015-0228) phase.

The deposition of $\text{Cu}(\text{ZnFe})\text{SnSe}_4$ at $300 \text{ }^\circ\text{C}$ gave only amorphous material which did not show any diffraction by p-XRD whereas uniform dark brownish films were obtained at $350 \text{ }^\circ\text{C}$. The p-XRD pattern of the thin films deposited at $350 \text{ }^\circ\text{C}$ are shown in Figure 2, peaks show clear shifts from Zn-rich $\text{Cu}_2\text{ZnFeSnS}_4$ (ICDD: 00-83-0225) and Fe-rich $\text{Cu}_2\text{ZnFeSnS}_4$ (ICDD: 01-015-0228) phase as expected. The p-XRD pattern found to be broader because of the small particle size of individual crystallites and overlapping of peaks especially about 2θ : 47 to 48° and around 2θ : 55 - 56 . The calculated lattice parameters from the p-XRD patterns was $a = 5.429(7) \text{ \AA}$ (Table 1).

A similar deposition with more Fe precursor concentration at $350 \text{ }^\circ\text{C}$ gave thin brown films. The p-XRD patterns were analysed by comparing with the Zn-rich $\text{Cu}_2\text{ZnFeSnS}_4$ (ICDD: 00-83-0225) an Fe-rich $\text{Cu}_2\text{ZnFeSnS}_4$ (ICDD: 01-015-0228) phases (Figure 2), It had been observed that the p-XRD patterns were shifted significantly from the reference patterns. The p-XRD patterns were further analysed using $\text{Cu}_2\text{FeSnSe}_4$ patterns (JCPDS: 00- 027-0167) but none of the peaks no matching peaks were seen. The calculated lattice parameters from the p-XRD patterns was $a = 5.492(7) \text{ \AA}$ (Table 1).

The deposition of $\text{Cu}_2(\text{ZnFe})\text{Sn}(\text{S}_x\text{Se}_{1-x})_4$ using a mixture of precursors as described in the experimental part gave only a negligible amount of deposits at $300 \text{ }^\circ\text{C}$ whereas good quality black specular films were deposited at $350 \text{ }^\circ\text{C}$. The p-XRD pattern of these films showed a clear shifts from those of the Fe-rich and Zn-rich phases of CZFTS indicating the formation of $\text{Cu}_2(\text{Zn}_y\text{Fe}_{1-y})\text{Sn}(\text{S}_x\text{Se}_{1-x})_4$ as shown in Figure 2. The calculated lattice parameter $a = 5.477(5) \text{ \AA}$ (Table 1). Another deposition with more Fe precursors at $350 \text{ }^\circ\text{C}$ produced thin black films. The p-XRD pattern was compared with Fe-rich ((ICDD: 01-015-0228) and Zn-rich ((ICDD 04-015-0225) CZFTS patterns. The peaks showed larger shift from both reference patterns (Figure 2). The lattice parameter a calculated from the p-XRD patterns was $5.429(8) \text{ \AA}$ (see Table 1).

SEM, EDX and TEM Studies

Elemental analysis of the films confirmed that the metal content of all films correlated well with mole fraction of metal in the feed shown in Figure 4. It is clear from the figure shows that a correlation between the mole fraction of Se in the precursor mixture and mole fraction of Se in the deposited thin films. From the graph it shows a

ARTICLE

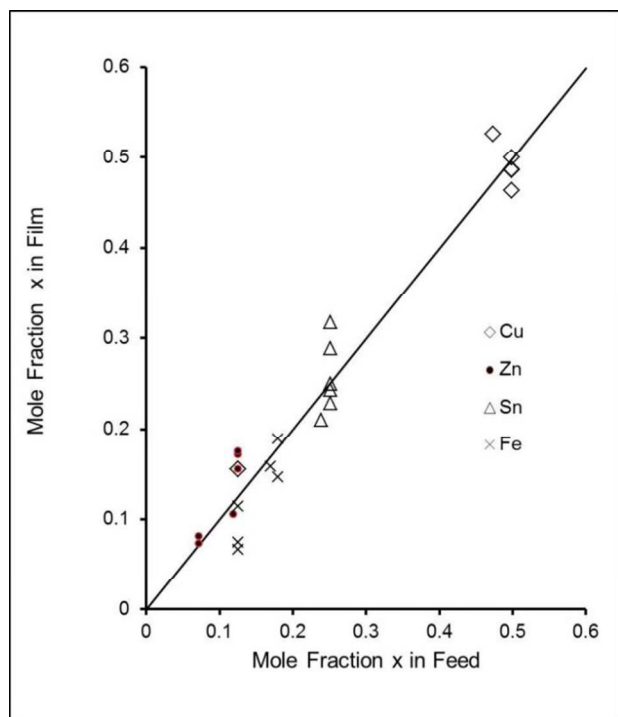


Figure 4: Correlation between mole fraction of each metal (x) in the feed and observed amount in the film by EDX

linear correlation between the mole fraction of Se in the precursor and in the deposited thin films

The SEM images of all deposited films showed different morphologies with $\sim 1\mu\text{m}$ thickness over the entire area of the substrate (Figure 5). Zn-rich phase of CZFTS thin films deposited at 350°C showed irregular flakes, less than 1 micron thickness. Elemental map confirmed of these films the uniform distribution of elements through the entire film (Figure 6(a)). EDX confirmed the p-XRD results by showing the deposition of the Zn-rich films: Cu (28.42%), Zn (8.84%), Fe (3.97%), Sn (15.23%), S (43.54%) corresponding to $\text{Cu}_{2.2}\text{Fe}_{0.3}\text{Zn}_{0.7}\text{Sn}_{1.2}\text{S}_{3.4}$. SEM images of the CZFTS thin films deposited from higher concentration of iron precursor showed uniform flakes with an even distribution (Figure 5(b)). EDX results revealed the composition as (Cu (25.92%) Zn (4.52%) Fe (9.5%) Sn (17.52%) S (45.54%)) giving an empirical formula of $\text{Cu}_{1.9}\text{Fe}_{0.7}\text{Zn}_{0.3}\text{Sn}_{1.3}\text{S}_{3.2}$ confirming the deposition of Fe-rich films. Elemental map of the films showed uniform composition of deposited material with constituent elements are shown in Figure 6(b).

The SEM images of C(ZF)TSe thin films deposited at 350°C showed irregular crystallites with size *ca.* $1\mu\text{m}$ as shown in

Figure 5(c). EDX analysis results showed atomic percentage of Cu (28.55%), Zn (10.72%), Fe (3.55%), Sn (14.50%) and Se (42.65%) which gave a stoichiometric composition as $\text{Cu}_{2.0}\text{Zn}_{0.7}\text{Fe}_{0.3}\text{Sn}_{1.0}\text{Se}_{3.1}$; a Zn-rich phase.

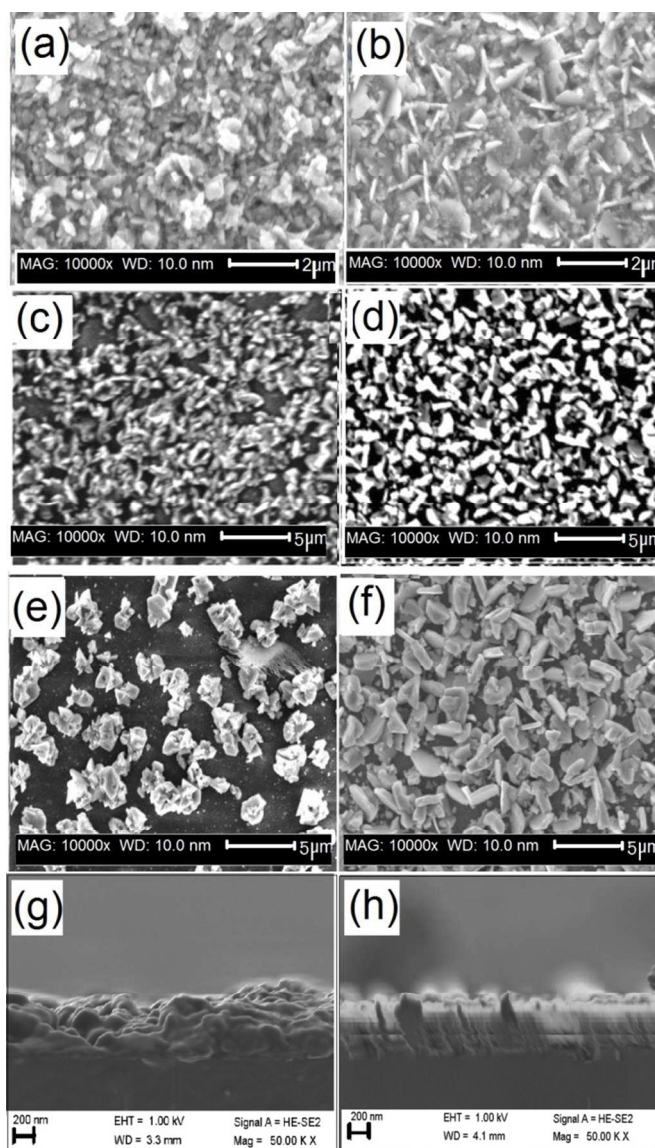


Figure 5: (a) and (b) are the SEM images, Zn-rich (CZFTS C1) and Fe-rich (CZFTS C2) phases of CZFTS films (c) and (d) are the SEM images, Zn-rich (CZFTSe C1) and Fe-rich (CZFTSe C2) phases of CZFTSe. (e) and (f) are the SEM images, Zn-rich (CZFTSSe C1) and Fe-rich (CSFTSSe C2) phases of CZFTSSe films deposited at 350°C . (g) and (h) are the cross sectional images of films (a) and (b).

SEM images with Fe-rich phases of C(ZF)TSe showed irregularly shaped crystallites (Figure 5(d)). EDX analysis showed atomic percentage of Cu (26.13%), Zn (4.10 %), Fe (11.21 %), Sn (13.60 %) and Se (44.13%) which gives a stoichiometric composition of $\text{Cu}_{1.8}\text{Zn}_{0.3}\text{Fe}_{0.7}\text{Sn}_{0.9}\text{Se}_{3.0}$ corresponding to Fe-rich phase.

The SEM images of $\text{Cu}_2(\text{ZnFe})\text{Sn}(\text{S}_x\text{Se}_{1-x})_4$ thin films deposited at 350 °C showed morphology based on irregular plate like crystallites as shown in Figure 5(e). The EDX analysis showed Cu (25.63%) Zn (8.74%) Fe (6.46%) Sn (12.46 %) S(28.74%) and Se (17.94 %) corresponding to $\text{Cu}_{1.7}\text{Fe}_{0.4}\text{Zn}_{0.6}\text{Sn}_{0.8}\text{S}_{1.9}\text{Se}_{1.2}$, the Zn-rich and S-rich stoichiometry.

The $(\text{ZnFe})\text{Sn}(\text{S}_x\text{Se}_{1-x})_4$ films deposited with higher concentration of Fe at 350 °C on EDX analysis showed Cu (26.87%) Zn (5.13 %) Fe (7.92%) Sn (11.15 %) S (26.24%) and Se (22.85 %) corresponding to $\text{Cu}_{2.1}\text{Fe}_{0.6}\text{Zn}_{0.4}\text{Sn}_{0.8}\text{S}_{2.1}\text{Se}_{1.7}$ which showed a Fe and S-rich stoichiometry. SEM images showed irregular plate like crystallites (Figure 5(f)). The elemental map showed uniform composition throughout the material (Supplementary material Figure S1 and S2).

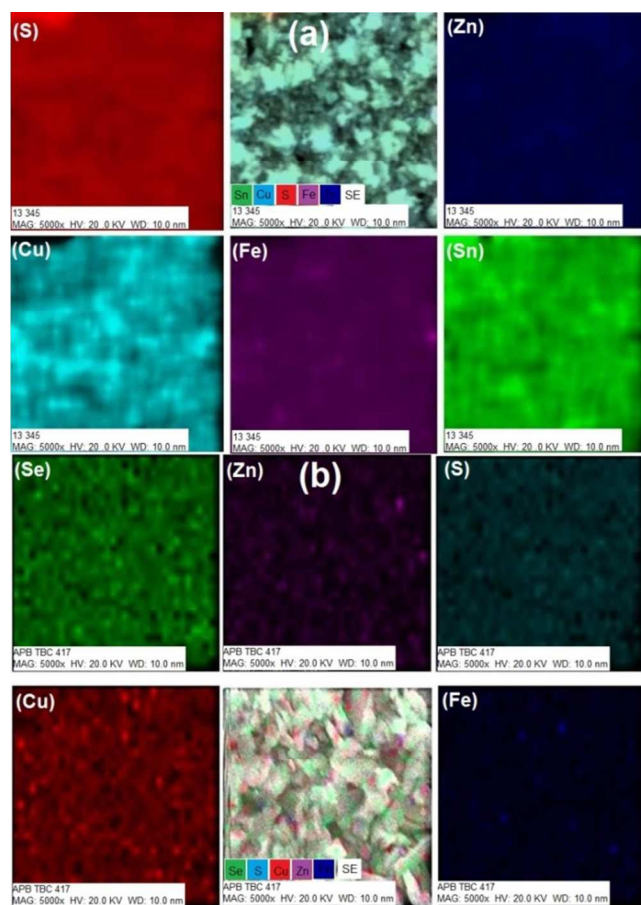


Figure 6: Elemental map images for (a) CZFTS C1 and (b) Zn-rich and Fe-rich (CZFTS C2) phases of CZFTS films deposited at 350 °C.

The Fe-rich CZFTS thin films (CZFTS C1) and Zn-rich (CZFTS C2) phases were further studied using TEM. The films were removed by scratching and ground, and dispersed in toluene for TEM analysis. The TEM images (Figure 7) showed flaky irregular crystallites with size ranging from 10 to 30 nm. Selected area elemental map results further revealed the Zn-rich and Fe-rich phases in the nm scale. The d-spacing obtained from lattice fringes and diffraction patterns were in good agreement with the standard patterns for the Zn-rich and Fe-rich phases.

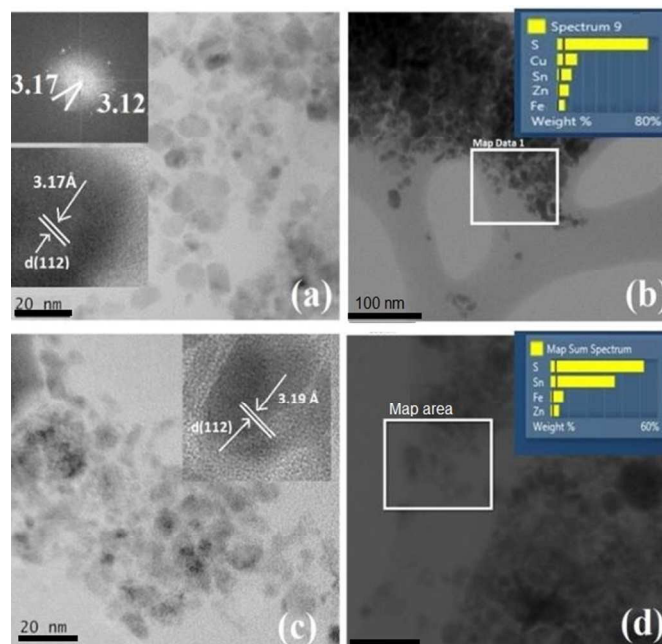


Figure 7: (a) and (b) shows the TEM images and elemental map of CZFTS thin films deposited using 2:0.5:0.5:1 molar ratio of Cu, Fe, Fe and Sn precursors at 350 °C (CZFTS C1). (c) and (d) shows the TEM and elemental maps of CZFTS thin films deposited with 2:0.7:0.3:1 molar ratio of Cu, Fe, Zn and Sn precursor mixture at 350 °C (CZFTS C2). Inserts images in (a) and (c) shows the d-spacing of the particles.

Raman Spectra and UV- Visible Spectra

The Raman spectra of films deposited with different [Fe]:[Zn] ratios of CZFTS, CZFTSe and CZFTSSe are shown in Figure 8. Raman spectra showed peaks at $\sim 340 \text{ cm}^{-1}$ and 350 cm^{-1} for CZFTS Fe-rich and Zn-rich phases. The Zn-rich CZFTS showed a higher Raman mode than the Fe-rich material as reported previously.^{2,7} Tauc plots drawn by plotting $(ah\nu)^2$ against $h\nu$ of films deposited with different [Fe]:[Zn] ratios of CZFTS, CZFTSe and CZFTSSe are shown in Supporting information Figure S3 which clearly show the variation in bandgaps. (Supporting information Table S3 and Table 1).

Raman spectra for the CZFTSSe films showed peaks at ~ 198 , 228 and $\sim 340 \text{ cm}^{-1}$. All these peaks are shifted from Raman peaks for CZFTSe (209 , 270 cm^{-1}) or CZFTS (321 , 284 , 218 cm^{-1}) phases as expected.^{7,8,26-28} Band gap measurements of CZFTS for Zn-rich

composition showed 1.72 eV whereas those with Fe-rich composition gave a band gap of 1.67 eV, which are close to those reported previously.^{2,7} Raman spectra obtained for the Fe-rich CZFTSe films showed a broad peak with low intensity at 230 cm⁻¹. The Zn-rich CZFTSe Raman shifts were observed at ~ 235 cm⁻¹ which lies between the end materials CZTSe and CFTSe phases with their corresponding Raman modes at 209 cm⁻¹ and 270 cm⁻¹ respectively.²⁷

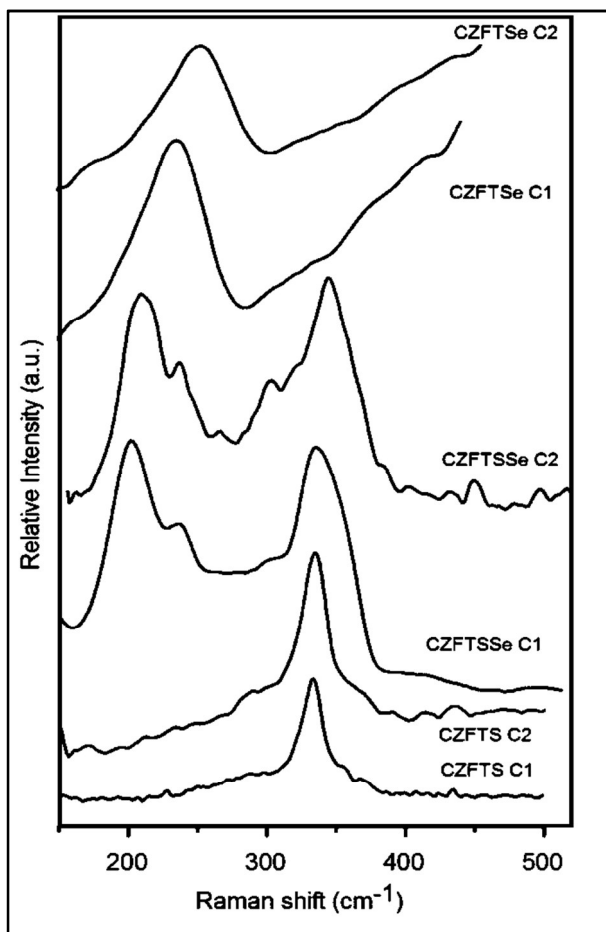


Figure 8: Raman spectra of Zn-rich and Fe-rich (C2CZFTS (CZFTS C1 and CZFTS C2), CZFTSe (CZFTSe C1 and CZFTSe C2) and CZFTSSe (CZFTSSe C1 and CZFTSSe C2) thin films deposited at 350 °C using different precursor mixtures.

Here also the Zn-rich phases showed slightly higher Raman mode as observed in CZFTS.^{2,7} The calculated band gaps were 1.48 and 1.47 eV for Zn-rich and Fe-rich CZFTSe thin films respectively which are in the range of CZTS, CZTSe, CZTSSe and CFTSe.²⁷⁻²⁹ UV/Vis Tauc plots drawn by plotting $(\alpha h\nu)^2$ against $h\nu$ gave a band gap values of ~1.64 and 1.61 eV for Zn-rich and Fe-rich CZFTSSe thin films, which were closer to that of the Kesterite CZFTS phases.^{2,6-8,14-20}

Electrical Sheet Resistance

Variation in the electrical sheet resistance with different Fe-compositions has been studied. The electrical resistance measured at

room temperature were 2.48 K Ω /sq for Fe-rich thin films and 2.42 K Ω /sq for Zn-rich films of CZFTS values which lie between the electrical sheet resistance for parent materials CZTS (2.8 K Ω /sq) and CFTS (2.3 K Ω /sq).^{9,28-31} The Fe-rich films showed comparatively lower resistance than the Zn-rich ones. The sheet resistance of the Zn-rich CZFTSe films and Fe-rich phases were observed as 2.10 K Ω /sq for and 2.07 K Ω /sq respectively, both values were lower than those for CZFTS (2.48 K Ω /sq and 2.42 K Ω /sq) as expected.

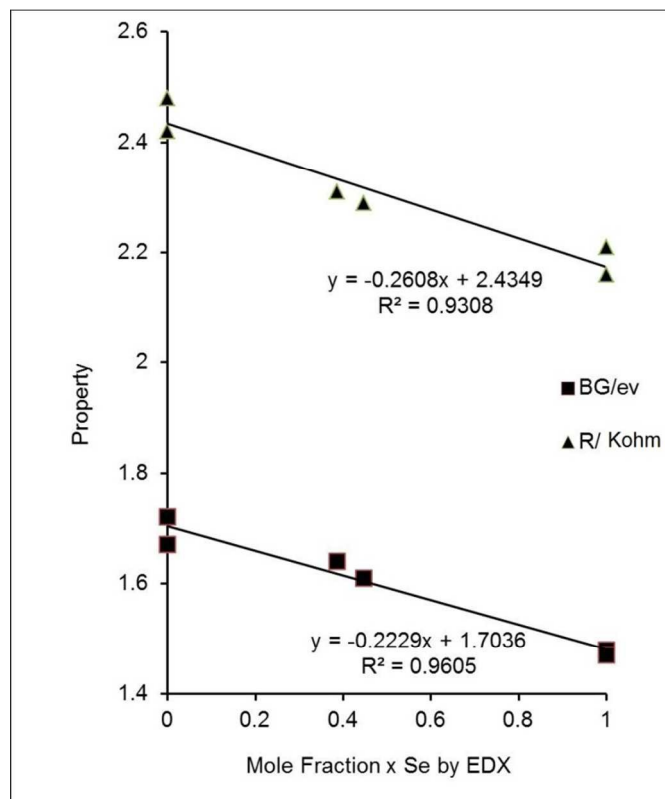


Figure 9: Vegard-type plot for resistance and band gaps of all samples against the mole fraction of Se as measured by EDX (band gap/eV, resistance/ K Ω /sq.)

The resistance value for end materials were as CZTSe (2.12 K Ω /sq) and CFTSe (2.04 K Ω /sq). These resistance measurements for CZFTSSe materials were found to be 2.31 and 2.29 K Ω /sq for Zn-rich and Fe-rich films respectively. Both values are lower than those of CZFTS Fe-rich (2.48 K Ω /sq) and Zn-rich phases (2.42 K Ω /sq) but higher than the CZFTSe Zn-rich (2.10 K Ω /sq) and Fe-rich (2.07 K Ω /sq) phases (Figure 10).^{32,33} (Supporting information Figure S4).

Vegard-type analysis were carried out using the measured band gap and sheet resistance values and is shown in Figure (9). There is a reasonable linear correlation between the Se/S mole fraction in all samples and these properties for all the films.

Conclusions

Thin films of CZFTS, CZFTSe and CZFTSSe have been deposited by AACVD. The ratios of the constituents: Zn, Fe, S and Se can be controlled by varying the concentrations of

corresponding precursors and the deposition temperature. The band gaps of these materials lie between 1.0 eV and 1.7 eV on changing the [Zn]:[Fe] and [S]:[Se] ratios in the material. These band gaps are ideal for absorber material in thin film solar cells. The sheet resistance of the materials are good for polycrystalline CZTS PV-cells. The structural parameters for the films do not show any consistent variation with composition, and given the wide range of differing radii of the ions involved this observation is perhaps not surprising. There is a distinct irregular trend following the mole fraction of selenium (Table 1). The band gap and resistance of each film is overwhelmingly controlled by the selenium content as shown in Figure 8. Dhurba and Kim have demonstrated the potential of such materials for solar cells.⁷ We now present a viable CVD method for their deposition. The potential for the use of these materials in devices will be investigated in the future.

Acknowledgements

We thank EPSRC for funding instruments, under grant number EP/K039547/1, used for characterization of compounds. PK thanks the School of Chemistry, The University of Manchester for funding.

Notes and references

^a School of Chemistry, The University of Manchester, Oxford Road M13 9PL

^b School of Materials, The University of Manchester, Oxford Road, M13 9PL

- D. B. Mitzi, O. Gunawan, T. K. Todorov, K. Wang, S. Guha, *Sol. Ener. Mater. and Solar Cells*, 2011, **95**, 1421-1436.
- G. L. Agawane, S. W. Shin, S. A. Vanalakar, A. V. Moholkar, J. H. Kim, *Mat. Lett.* 2014, **137**, 147-149.
- X. Fontane, V. Izquierdo-Roca, E. Saucedo, S. Schorr, V. O. Yukhymchuk, M. Y. Valakh, M. Y., et al. *J. Alloys Compd.* 2012, **539**, 190-194
- P. Bonazzi, L. Bindi, G. P. Bernardini, S. Menchetti, *Can. Miner.* 2003, **41**, 639
- T. Shibuya, Y. Goto, Y. Kamihara, M. Matoba, K. Yasuoka, L. A. Burton, A. Walsh, *Appl. Phys. Lett.* 2014, **104**, 021912.
- S. R. Hall, J. T. Szymanski, J. M. Stewart, *Can. Miner.* 1978, **16**, 131-137.
- D. B. Khadka, J. J. Kim, *Phys. Chem. C*, 2014, **118**, 14227.
- S. H. Chang, M. Y. Chiang, C. C. Chiang, F. W. Yuan, C. Y. Chen, B. C. Chiu, T. L. Kao, C. H. Lai, H. Y. Tuan, *Ener. Environ. Sci.*, 2011, **4**, 4929-4932.
- (a) P. Marchand, I. A. Hassan, I. P. Parkin, C. J. Carmalt, *Dalton Trans.*, 2013, **42**, 9406-9422 (b) M. Nyman, M. J. Hampden-Smith, E. A. Duesler, *Chem. Vap. Deposition*. 1996, **2**, 171-173
- M. N. McCain, S. Schneider, M. R. Salata, T. J. Marks, *Inorg. Chem.* 2008, **47**, 2534-2542.
- (a) C. R. Crick, I. P. Parkin, *J. Mater. Chem.*, 2009, **19**, 1074-1076; (b) M. R. Waugh, G. Hyett, I. P. Parkin, *Chem. Vap. Deposition* 2008, **14**, 366-372
- K. G. U. Wijayantha, S. Saremi-Yarahmadia, L. M. Peter, *Phys. Chem. Chem. Phys.*, 2011, **13**, 5264-5270
- A. A. Tahir, M. Mazhar, M. Hamid, K. G. U. Wijayantha, K. C. Molloy, *Dalton Trans.*, 2009, **19**, 3674-3680
- A. A. Tahir, K. G. U. Wijayantha, S. Saremi-Yarahmadia, M. Mazhar, V. McKee, *Chem. Mater.* 2009, **21**, 3763-3772
- (a) K. Ramasamy, V. L. Kuznetsov, K. Gopal, M. A. Malik, J. Raftery, P. Edwards, P. O'Brien, *Chem. Mater.* 2013, **25**, 266-276K. (b) P. Kevin, D. J. Lewis, J. Raftery, M. A. Malik, P. O'Brien, *J. Cryst. Growth*, 2015, **415**, 93-99.
- K. Ramasamy, M. A. Malik, P. O'Brien, *Chem. Sci.* 2011, **2**, 1170.
- S. Mahboob, S. N. Malik, N. Haider, C. Q. Nguyen, M. A. Malik, P. O'Brien, *J. Cryst. Growth*, 2014, **394**, 39
- A. Adeogun, M. Afzaal and P. O'Brien, *Chem. Vap. Deposition*, 2006, **12**, 597-599.
- (a) D. J. Lewis, P. O'Brien, *Chem. Commun.* 2014, **50**, 6319; (b) P. Kevin, S. N. Malik, M. A. Malik, P. O'Brien, *Chem. Commun.*, 2014, **50**, 14328-14330.
- R. A. Hussain, A. Badshah, M. Dilshad Khan, N. Haider, Bhajan Lal, S. Ishtiaq Khan, A. Shah, *Mater. Chem. and Phys.*, 2015, **30**, 1-7.
- P. Brack, J. S. Sagu, T. A. N. Peiris, A. McInnes, M. Senili, K. G. U. Wijayantha, F. Marken, E. Selli, *Chem. Vap. Deposition* 2015, **21**, 41-45.
- M. A. Ehsan, T. A. Nirmal Peiris, K. G. U. Upul Wijayantha, M. M. Olmstead, Z. Arifin, M. Mazhar, K. M. Loa, V. McKee, *Dalton Trans.*, 2013, **42**, 10919-10928.
- N. Revaprasadu, M. A. Malik, P. O'Brien, *J. Mater. Res.*, 1999, **14**, 3237; M. A. Malik, M. Motevalli and P. O'Brien, *Inorg. Chem.* 1995, **34**, 6223; M. A. Malik, M. Motevalli, P. O'Brien and J. R. Walsh, *Organometallics* 1992, **11**, 3136; A. A. M. Memon, M. Afzaal, M. A. Malik, C. Nguyen, P. O'Brien, J. Raftery, *Dalton Trans.* 2006, 4499; D. J. Binks, S. P. Bants, D. P. West, M. A. Malik, P. O'Brien, *J. Mod. Optic.* 2003, **50**, 299.; C. Q. Nguyen, A. E. Adeogun, M. Afzaal, M. A. Malik and P. O'Brien, *Chem. Commun.*, 2006, 2182; M. A. Malik, M. Motevalli, T. Saeed and P. O'Brien, *Adv. Mater.*, 1993, **5**, 653; A. Panneerselvam, C. Q. Nguyen, M. A. Malik, P. O'Brien, J. Raftery *J. Mater. Chem.* 2009, **19**, 419-427; Revaprasadu, N.; Malik, M. A.; O'Brien, *South African J. Chemistry* 2004, **57**, 40-43.
- M. Akhtar, J. Akhter, M. A. Malik, P. O'Brien, P. F. Tuna, J. Raftery, M. Helliwell, M. *Journal of Materials Chemistry*, 2011, **21**, 9737-9745;
- M. B. Hursthouse, M. A. Malik, M. Motevalli, M. P. O'Brien, *J. Mater. Chem.*, 1992, **2**, 949
- E. S. Schorr, V. O. Yukhymchuk, M. Y. Valakh, A. Pérez-Rodríguez, J. R. Morante, *J. Alloys and Compounds*, 2012, **539**, 190-194.
- M. Cao, B. L. Zhang, J. Huang, Y. Sun, L. J. Wang, Y. Shen, *Chem. Phys. Lett.* 2014, **604**, 15-21.
- S. C. Riha, B. A. Parkinson, A. L. Prieto, *J. Am. Chem. Soc.*, 2011, **133**, 15272-15275.
- C. Jiang, J. S. Lee, D. V. Talapin, *J. Am. Chem. Soc.*, 2012, **134**, 5010-5013
- X. Zhang, N. Bao, K. Ramasamy, Y. H. A. Wang, Y. Wang, B. Lin, A. Gupta, *Chem. Commun.*, 2012, **48**, 4956

- 31 H. Katagiri, K. Saitoh, T. Washio, H. Shinohara, T. Kurumadani, S. Miyajima, *Sol. Energy. Mater Sol. Cells* 2001, **65**, 141-148
- 32 X. Yu, A. Ren, F. Wang, C. Wang, J. Zhang, W. Wang, L. Wu, W. Li, G.Zeng, L. Feng, *Int. J. Photoenergy*, 2014 , **6**, 1-9
- 33 E.M. Mkawi, K. Ibrahim, M. K. M. Ali, A. S. Mohamed, *Int. J. Electrochem. Sci*, 2013, **8**, 359 – 368.

Graphical Abstract

The Deposition of
 $\text{Cu}_2(\text{Zn}_y\text{Fe}_{1-y})\text{SnS}_4$,
 $\text{Cu}_2(\text{Zn}_y\text{Fe}_{1-y})\text{SnSe}_4$ and
 $\text{Cu}_2(\text{Zn}_y\text{Fe}_{1-y})\text{Sn}(\text{S}_x\text{Se}_{1-x})_4$
Thin Films by AACVD:
Potential Solar Cell
Materials based on Earth
Abundant Elements
Punarja Kevin,
Mohammad Azad Malik,
Paul O'Brien

